



## **Simultaneous multislice echo planar imaging with blipped controlled aliasing in parallel imaging results in higher acceleration: a promising technique for accelerated diffusion tensor imaging of skeletal muscle**

Filli, Lukas ; Piccirelli, Marco ; Kenkel, David ; Guggenberger, Roman ; Andreisek, Gustav ; Beck, Thomas ; Runge, Val M ; Boss, Andreas

**Abstract:** **PURPOSE** The aim of this study was to investigate the feasibility of accelerated diffusion tensor imaging (DTI) of skeletal muscle using echo planar imaging (EPI) applying simultaneous multislice excitation with a blipped controlled aliasing in parallel imaging results in higher acceleration unaliasing technique. **MATERIALS AND METHODS** After federal ethics board approval, the lower leg muscles of 8 healthy volunteers (mean [SD] age, 29.4 [2.9] years) were examined in a clinical 3-T magnetic resonance scanner using a 15-channel knee coil. The EPI was performed at a b value of 500 s/mm without slice acceleration (conventional DTI) as well as with 2-fold and 3-fold acceleration. Fractional anisotropy (FA) and mean diffusivity (MD) were measured in all 3 acquisitions. Fiber tracking performance was compared between the acquisitions regarding the number of tracks, average track length, and anatomical precision using multivariate analysis of variance and Mann-Whitney U tests. **RESULTS** Acquisition time was 7:24 minutes for conventional DTI, 3:53 minutes for 2-fold acceleration, and 2:38 minutes for 3-fold acceleration. Overall FA and MD values ranged from 0.220 to 0.378 and 1.595 to 1.829 mm/s, respectively. Two-fold acceleration yielded similar FA and MD values ( $P = 0.901$ ) and similar fiber tracking performance compared with conventional DTI. Three-fold acceleration resulted in comparable MD ( $P = 0.199$ ) but higher FA values ( $P = 0.006$ ) and significantly impaired fiber tracking in the soleus and tibialis anterior muscles (number of tracks,  $P < 0.001$ ; anatomical precision,  $P = 0.005$ ). **CONCLUSIONS** Simultaneous multislice EPI with blipped controlled aliasing in parallel imaging results in higher acceleration can remarkably reduce acquisition time in DTI of skeletal muscle with similar image quality and quantification accuracy of diffusion parameters. This may increase the clinical applicability of muscle anisotropy measurements.

DOI: <https://doi.org/10.1097/RLI.0000000000000151>

Posted at the Zurich Open Repository and Archive, University of Zurich

ZORA URL: <https://doi.org/10.5167/uzh-110272>

Journal Article

Published Version

Originally published at:

Filli, Lukas; Piccirelli, Marco; Kenkel, David; Guggenberger, Roman; Andreisek, Gustav; Beck, Thomas; Runge, Val M; Boss, Andreas (2015). Simultaneous multislice echo planar imaging with blipped controlled aliasing in parallel imaging results in higher acceleration: a promising technique for accelerated diffusion tensor imaging of skeletal muscle. *Investigative Radiology*, 50(7):456-463.

DOI: <https://doi.org/10.1097/RLI.0000000000000151>

# Simultaneous Multislice Echo Planar Imaging With Blipped Controlled Aliasing in Parallel Imaging Results in Higher Acceleration

## *A Promising Technique for Accelerated Diffusion Tensor Imaging of Skeletal Muscle*

Lukas Filli, MD,\* Marco Piccirelli, PhD,† David Kenkel, MD,\* Roman Guggenberger, MD,\* Gustav Andreisek, MD, MBA,\* Thomas Beck, PhD,‡ Val M. Runge, MD,\* and Andreas Boss, MD, PhD\*

**Purpose:** The aim of this study was to investigate the feasibility of accelerated diffusion tensor imaging (DTI) of skeletal muscle using echo planar imaging (EPI) applying simultaneous multislice excitation with a blipped controlled aliasing in parallel imaging results in higher acceleration unaliasing technique.

**Materials and Methods:** After federal ethics board approval, the lower leg muscles of 8 healthy volunteers (mean [SD] age, 29.4 [2.9] years) were examined in a clinical 3-T magnetic resonance scanner using a 15-channel knee coil. The EPI was performed at a  $b$  value of 500 s/mm<sup>2</sup> without slice acceleration (conventional DTI) as well as with 2-fold and 3-fold acceleration. Fractional anisotropy (FA) and mean diffusivity (MD) were measured in all 3 acquisitions. Fiber tracking performance was compared between the acquisitions regarding the number of tracks, average track length, and anatomical precision using multivariate analysis of variance and Mann-Whitney  $U$  tests.

**Results:** Acquisition time was 7:24 minutes for conventional DTI, 3:53 minutes for 2-fold acceleration, and 2:38 minutes for 3-fold acceleration. Overall FA and MD values ranged from 0.220 to 0.378 and 1.595 to 1.829 mm<sup>2</sup>/s, respectively. Two-fold acceleration yielded similar FA and MD values ( $P \geq 0.901$ ) and similar fiber tracking performance compared with conventional DTI. Three-fold acceleration resulted in comparable MD ( $P = 0.199$ ) but higher FA values ( $P = 0.006$ ) and significantly impaired fiber tracking in the soleus and tibialis anterior muscles (number of tracks,  $P < 0.001$ ; anatomical precision,  $P \leq 0.005$ ).

**Conclusions:** Simultaneous multislice EPI with blipped controlled aliasing in parallel imaging results in higher acceleration can remarkably reduce acquisition time in DTI of skeletal muscle with similar image quality and quantification accuracy of diffusion parameters. This may increase the clinical applicability of muscle anisotropy measurements.

**Key Words:** diffusion tensor imaging, diffusion tractography, muscle skeletal, simultaneous multislice, echo planar imaging

(Invest Radiol 2015;00: 00–00)

Diffusion tensor magnetic resonance imaging (DTI) is based on measuring the molecular diffusion along 6 or more different directions. It is based on the fact that the diffusion in the body is constrained by cellular barriers and thus anisotropic in organized tissue.<sup>1</sup> The eigenvectors of the diffusion tensor and their respective eigenvalues, the fractional anisotropy (FA), and the mean diffusivity (MD) are DTI metrics that can be calculated voxelwise. By connecting voxels with similar characteristics in series, fiber tracking algorithms allow 3-dimensional visualization of the fiber course.<sup>2–5</sup>

Many physiological studies confirmed that the first eigenvalue represents the main diffusion direction in skeletal muscle fibers.<sup>6–10</sup> With its long, parallel running fibers, skeletal muscle is an ideal tissue for DTI applications. Examples include the characterization of changes after exercise or pathological changes such as muscle edema, tear, or hematoma.<sup>11–16</sup>

Diffusion tensor magnetic resonance imaging of the muscle is inherently limited by the short T2 relaxation time of skeletal muscle (around 35 milliseconds at 3 T)<sup>17</sup> and the resulting low signal-to-noise ratio (SNR).<sup>18</sup> It can be further hampered by artifacts because of motion, blood pulsation, or table vibration during the image acquisition. The relatively low SNR of muscle DTI compared with other body areas (such as the brain) needs to be compensated by an increased number of acquisitions for averaging. The long acquisition time currently limits the clinical applicability of muscle DTI. Diffusion tensor magnetic resonance imaging is usually performed based on single-shot echo planar imaging (EPI). Conventional acceleration techniques such as parallel imaging<sup>19</sup> or partial Fourier acquisition<sup>20</sup> only allow shorter echo time (TE) but do not act on the number of acquisitions or the repetition time (TR) in single-shot EPI. An alternative approach for accelerated imaging is simultaneous multislice (SMS) imaging, where multiple slices are excited by a single radiofrequency pulse (ie, a multiband pulse). This approach has become promising because of recent technical advances such as controlled aliasing in parallel imaging results in higher acceleration (CAIPIRINHA) unaliasing technique<sup>21</sup> and its implementation to EPI with markedly reduced g-factor SNR penalty (blipped CAIPIRINHA).<sup>22–24</sup>

Simultaneous multislice has already proven useful in accelerated cardiac DTI.<sup>25</sup> In the present study, the feasibility and accuracy of this technique for in vivo imaging of skeletal muscle was tested on the lower legs. We hypothesized that, despite a significantly reduced acquisition time, the image quality and quantification accuracy of simultaneous multislice DTI with blipped CAIPIRINHA would not be statistically significantly different compared with conventional DTI.

## MATERIALS AND METHODS

### Study Population

After approval by the federal ethics board, this study was performed on the calf of 8 consecutive healthy subjects (6 males, 2 females; mean [SD] age, 29.4 [2.9] years). All subjects gave written informed consent to the magnetic resonance examination and the scientific use of the data. None of the subjects reported previous surgery or major trauma to the examined extremity.

### Imaging Protocol

All images were acquired on a 3-T scanner (Magnetom Skyra, Siemens Healthcare, Erlangen, Germany) featuring a maximum gradient field amplitude of 45 mT/m and a slew rate of 200 T/m/s. The subjects were positioned supine with their legs (5 right side, 3 left side) placed parallel to the main magnetic field in a dedicated 15-channel transmit/receive knee coil.

Received for publication November 28, 2014; and accepted for publication, after revision, February 2, 2015.

From the \*Institute of Diagnostic and Interventional Radiology and †Department of Neuroradiology, University Hospital Zurich, University of Zurich, Zurich, Switzerland; and ‡MR Application Development, Siemens Healthcare, Erlangen, Germany.

Conflicts of interest and sources of funding: none declared.

Reprints: Lukas Filli, MD, Institute of Diagnostic and Interventional Radiology, University Hospital Zurich, University of Zurich, Raemistrasse 100, CH-8091 Zurich, Switzerland. E-mail: Lukas.Filli@usz.ch.

Copyright © 2015 Wolters Kluwer Health, Inc. All rights reserved.  
ISSN: 0020-9996/15/0000-0000

First, a 3-dimensional encoded fast spin-echo T1-weighted axial sequence (SPACE sequence, sampling perfection with application of optimized contrasts using different flip angle evolution; TR, 500 milliseconds; TE, 11 milliseconds; turbo factor, 42; number of slices, 192; slice thickness, 1.0 mm; field of view,  $16 \times 16 \text{ cm}^2$ ; in-plane resolution,  $0.5 \times 0.5 \text{ mm}^2$ ) was acquired at the level of the proximal third of the calf for anatomical reference and to exclude structural pathologies, which would have influenced quantitative evaluation of DTI parameters or fiber tracking. Next, DTI was performed using a single-shot EPI sequence with 20 different gradient directions at a  $b$  value of  $500 \text{ s/mm}^2$ , which has proven the optimal value for DTI of skeletal muscle.<sup>26</sup> Simultaneous multislice acquisition with blipped CAIPIRINHA was achieved with dedicated software for research purposes (Siemens Healthcare, Erlangen, Germany).

Different scans were performed with no slice acceleration (ie, conventional DTI; TR, 6100 milliseconds), 2-fold acceleration (2 slices excited with 1 pulse and readout simultaneously; TR, 3100 milliseconds), and 3-fold acceleration (3 slices excited with 1 pulse and readout simultaneously; TR, 2100 milliseconds). Except for TR, all parameters were kept constant (TE, 54 milliseconds; voxel dimensions,  $1.4 \times 1.4 \times 3 \text{ mm}^3$ ; field of view,  $150 \times 150 \text{ mm}^2$ ; slices, 57; slice gap, 0; signal averages, 3; partial Fourier acquisition, 5/8; generalized autocalibrating partially parallel acquisition 2; bandwidth, 1228 Hz/Px). Each DTI sequence was acquired twice to calculate the SNR and the reproducibility (see below).

### Postprocessing and Quantitative DTI Evaluation

The postprocessing routine of the EPI sequence automatically generated grayscale FA and MD maps as well as color-coded FA

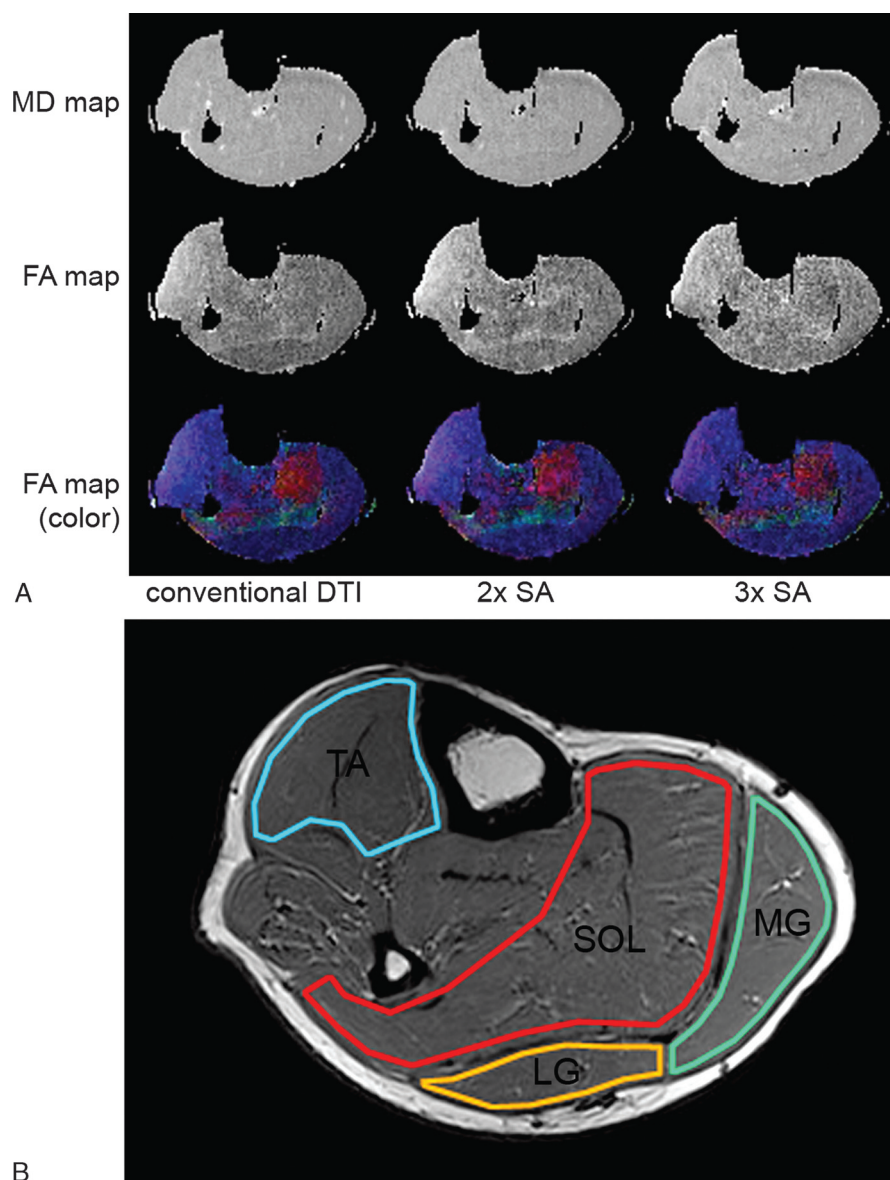


**FIGURE 1.** A, MD and FA maps at the level of the maximum diameter of the right calf of a 29-year-old male volunteer. On the color-coded FA maps, the red channel is assigned to the transversal axis, the green channel to the sagittal axis, and the blue channel to the longitudinal axis (z axis) of the scanner. Because the muscle fibers are predominantly directed along the z axis, blue is the dominant color. SA indicates slice acceleration. B, Corresponding T1-weighted image illustrating ROI placement in the different muscles (MG/LG, medial and lateral head of the gastrocnemius muscle; SOL, soleus muscle; TA, TA muscle).

maps that contained 3-dimensional information on the voxelwise diffusion orientation. Fractional anisotropy and MD were measured by 2 independent radiologists (initials blinded) at the level of the maximum calf diameter, which was identified on the T1-weighted images. Polygonal regions of interest (ROIs) were placed in the medial and lateral head of the gastrocnemius muscle, the soleus muscle, and the tibialis anterior (TA) muscle.<sup>9,27</sup> The ROIs were defined slightly smaller than the cross-sectional area of the muscles to avoid partial volume effects and the inclusion of fat or blood vessels (Fig. 1).

## Fiber Tracking

Tracking of muscle fibers was performed by 1 reader (initials blinded, with 4 years of experience in muscle DTI) using a dedicated postprocessing unit and software (Neuro 3D application; syngo Leonardo, Siemens Healthcare, Erlangen, Germany). In all DTI sequences, seed ROIs were drawn on the b0 image in each muscle at the level of the maximum calf diameter. Automated continuous fiber tracking then started from these ROIs. If a voxel's characteristics fell below the FA threshold of less than 0.15 or exceeded the angulation threshold greater than 30 degrees relative to the voxel tracked before, fiber tracking automatically stopped at the level of that voxel.

The performance of fiber tracking depending on the slice acceleration was assessed by the same reader regarding the number of tracks and average track length in the different muscles. In addition, a 5-point qualitative rating was performed regarding the anatomical precision of the tracks (1, poor; 2, fair; 3, substantial; 4, good; 5, excellent).

## Calculation of the SNR

All DTI sequences with different acceleration factors were acquired twice in every volunteer. By subtracting corresponding sequences at  $b = 0$ , voxel-based difference images could be generated.<sup>28,29</sup> On

the difference images, the SD of the signal intensity (SI), that is, the effective image noise, was measured. The respective SIs of the different muscles were measured at the level of the maximum calf diameter. The effective SNR was then calculated separately for all muscles<sup>28</sup> as follows:

$$SNR = \frac{SI \times \sqrt{2}}{SD} \quad (1)$$

In addition, the SNR per minute was calculated by dividing the SNR value of each sequence by its acquisition time.

## Statistical Analysis

Statistical analysis was performed using SPSS (version 20, IBM Corp, Somers, NY). The interobserver agreement for FA and MD measurements was assessed by calculating respective intraclass correlation coefficients (ICCs). Intraclass correlation coefficients were interpreted according to Landis and Koch.<sup>30</sup> Average FA and MD values from both readers were calculated for further statistical comparisons.

Multivariate analysis of variance with post hoc Bonferroni tests was used to compare the sequences with different slice acceleration factors regarding FA and MD values and fiber tracking parameters (number of tracks, average track length). Anatomical precision scores of fiber tracking in the different sequences and muscles were compared using Mann-Whitney  $U$  tests. For all tests, a  $P$  value less than 0.05 was considered statistically significant. In addition, FA and MD values measured on the slice-accelerated sequences were compared with those measured on the conventional DTI sequence by using Bland-Altman plots.

The coefficient of variation (SD divided by the mean) was calculated for FA and MD for each sequence. Furthermore, the double acquisition of all DTI sequences allowed a reproducibility

**TABLE 1.** FA and MD Measured in the MG/LG, SOL, and TA Muscles by 2 Independent Readers

Muscle	ROI Size, cm <sup>2</sup>	Conventional DTI (No Slice Acceleration)		Two-Fold Slice Acceleration		Three-Fold Slice Acceleration	
		FA	MD (10 <sup>−3</sup> mm <sup>2</sup> /s)	FA	MD (10 <sup>−3</sup> mm <sup>2</sup> /s)	FA	MD (10 <sup>−3</sup> mm <sup>2</sup> /s)
Reader 1							
MG	10.35 (2.87)	0.219 (0.014)	1.596 (0.064)	0.226 (0.014)	1.576 (0.075)	0.241 (0.017)	1.589 (0.080)
LG	7.68 (1.48)	0.230 (0.020)	1.659 (0.049)	0.239 (0.019)	1.625 (0.083)	0.244 (0.013)	1.661 (0.079)
SOL	13.54 (1.81)	0.235 (0.019)	1.639 (0.054)	0.228 (0.015)	1.616 (0.049)	0.262 (0.029)	1.628 (0.051)
TA	8.44 (1.31)	0.339 (0.030)	1.721 (0.071)	0.351 (0.028)	1.689 (0.105)	0.370 (0.033)	1.808 (0.068)
Reader 2							
MG	10.78 (4.85)	0.221 (0.018)	1.636 (0.153)	0.230 (0.023)	1.615 (0.163)	0.244 (0.025)	1.639 (0.185)
LG	7.78 (2.88)	0.217 (0.012)	1.691 (0.122)	0.229 (0.019)	1.662 (0.177)	0.238 (0.025)	1.701 (0.175)
SOL	13.32 (2.92)	0.236 (0.044)	1.686 (0.161)	0.226 (0.034)	1.658 (0.141)	0.272 (0.064)	1.677 (0.145)
TA	8.78 (2.7)	0.355 (0.074)	1.761 (0.161)	0.361 (0.071)	1.739 (0.198)	0.386 (0.085)	1.849 (0.162)
Both readers							
MG	10.54 (3.68)	0.220 (0.014)	1.616 (0.093)	0.228 (0.016)	1.595 (0.043)	0.242 (0.017)	1.614 (0.120)
LG	7.73 (1.93)	0.224 (0.015)	1.675 (0.062)	0.234 (0.016)	1.644 (0.102)	0.241 (0.015)	1.681 (0.102)
SOL	13.43 (2.01)	0.235 (0.029)	1.663 (0.097)	0.227 (0.021)	1.637 (0.083)	0.267 (0.040)	1.652 (0.085)
TA	8.61 (1.86)	0.347 (0.048)	1.741 (0.099)	0.356 (0.048)	1.714 (0.139)	0.378 (0.057)	1.829 (0.098)
ICC (95% confidence interval)							
Total	0.772 (0.530–0.889)	0.836 (0.691–0.917)	0.687 (−0.317–0.834)	0.847 (0.758–0.937)	0.647 (0.299–0.876)	0.890 (0.775–0.946)	0.649 (0.297–0.827)

FA indicates fractional anisotropy; MD, mean diffusivity; MG, medial head of the gastrocnemius; LG, lateral head of the gastrocnemius; SOL, soleus; ROI, region of interest; DTI, diffusion tensor magnetic resonance imaging; TA, tibialis anterior; ICC, intraclass correlation coefficient.



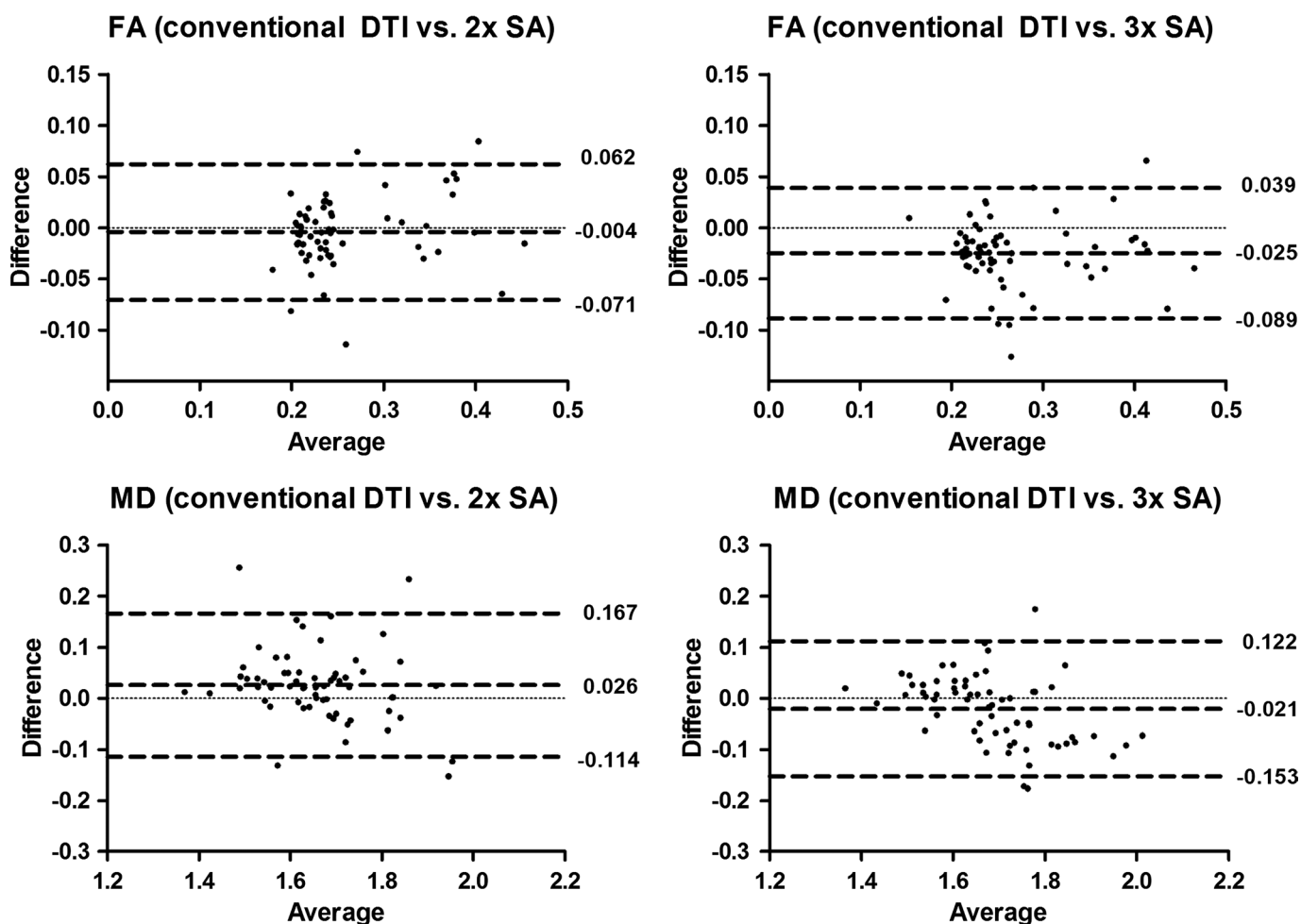


**FIGURE 2.** Bland-Altman plots illustrating the agreement between conventional DTI and slice-accelerated sequences. As to FA, almost no bias occurred between conventional DTI and 2-fold acceleration, whereas 3-fold acceleration led to a systematic bias of  $-0.025$ . Compared with conventional DTI, MD was slightly overestimated in 2-fold acceleration and slightly underestimated in 3-fold acceleration.

assessment of the diffusion tensor parameters (FA, MD) by calculating respective ICCs.

## RESULTS

### Image Acquisition

Image acquisition was successful in all subjects. The acquisition time was 7:24 minutes without slice acceleration (conventional DTI), 3:53 minutes with 2-fold slice acceleration, and 2:38 minutes with 3-fold slice acceleration. The entire protocol took 34 minutes. The specific absorption rate remained below 20% of the allowed maximum in all DTI sequences and volunteers, and switching to first level acquisition mode was not necessary.

### Quantitative Measurements

Fractional anisotropy and MD values measured in the different muscle groups are provided in Table 1. The interobserver agreement was “almost perfect” for FA values (ICC, 0.836–0.890) and “substantial” for MD values (ICC, 0.647–0.687) and ROI sizes (ICC, 0.772).<sup>30</sup>

Multivariate analysis of variance with post hoc Bonferroni tests revealed significantly higher FA ( $P < 0.001$ ) and MD ( $P \leq 0.009$ ) values in the TA muscle than in the other muscles. No significant

differences in terms of FA and MD were found between the lateral gastrocnemius, medial gastrocnemius, and soleus muscles.

Two-fold slice acceleration yielded similar FA and MD values compared with conventional DTI ( $P \geq 0.901$ ). Three-fold slice acceleration induced comparable MD values ( $P = 0.199$ ) but significantly higher FA values ( $P = 0.006$ ) compared with conventional DTI. This finding is confirmed by the corresponding Bland-Altman plot, which showed a systematic FA bias of  $-0.025$  (Fig. 2).

The coefficients of variation in the different muscles were similarly low in all sequences for FA (no slice acceleration, 6.2%–13.9%; 2-fold acceleration, 6.8%–13.4%; 3-fold acceleration, 6.4%–15.0%) and MD (no slice acceleration, 3.7%–5.8%; 2-fold acceleration, 5.1%–8.1%; 3-fold acceleration, 5.2%–7.4%). The reproducibility of DTI measures was almost perfect in all sequences (FA: ICCs, 0.827–0.872; MD: ICCs, 0.837–0.919).

### Fiber Tracking

Fiber tracking was successfully performed in all subjects (example 3-dimensional images are shown in Fig. 3). Compared with conventional DTI, 2-fold slice acceleration did not have any significant influence on the measured number of tracks ( $P \geq 0.151$ ), the average track length ( $P \geq 0.346$ ), or the qualitative anatomical precision score ( $P \geq 0.234$ ) in the different muscles. The same was observed for

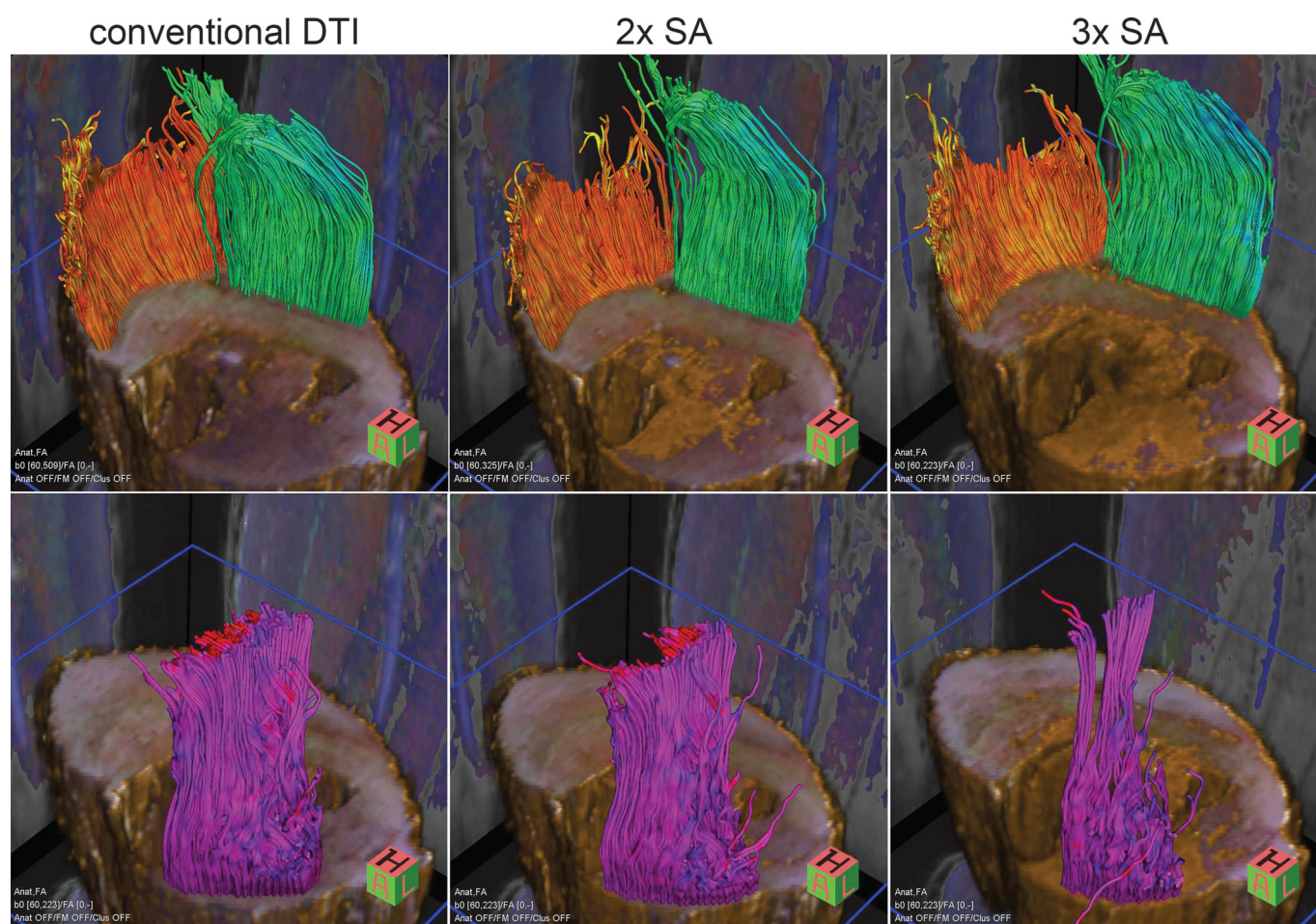


**FIGURE 3.** Examples of 3-dimensional images of fiber tracking in conventional DTI as well as with 2-fold and 3-fold slice acceleration (SA). Seed ROIs were placed in the different muscles at the level of the maximum calf diameter. Although fiber tracking worked well in all 3 scenarios in the medial (orange) and lateral (cyan) head of the gastrocnemius muscle, fewer fibers could be tracked in the TA muscle (pink) with increasing slice acceleration, which can be explained with the decreasing SNR.

3-fold acceleration in the medial and lateral gastrocnemius muscles; however, in the soleus and TA muscles, a significant decrease in the number of tracks ( $P < 0.001$ ) and the anatomical precision score ( $P \leq 0.005$ ) was found. Three-fold acceleration did not have any significant influence on the average track length (medial gastrocnemius,  $P = 0.322$ ; lateral gastrocnemius,  $P = 0.902$ ; soleus,  $P = 0.655$ ; TA,  $P = 0.117$ ) (Fig. 4).

### Signal-to-Noise Ratio

Signal-to-noise ratio values in the different muscles at different slice acceleration are provided in Table 2. The overall SNR values were 57.31 (SD, 6.63) (conventional DTI), 45.25 (11.22) (2-fold slice acceleration), and 35.12 (8.24) (3-fold slice acceleration), respectively. In all muscle groups, the SNR per minute increased with higher slice acceleration (Table 2).

### DISCUSSION

Diffusion tensor magnetic resonance imaging of skeletal muscle has proven useful not only for illustration of the physiological fiber course but also for the characterization of muscle pathologies.<sup>11–13</sup> Currently, its applicability in clinical routine is mainly limited by incoherent motion (and concomitant signal drop) arising from muscle motion,

blood pulsation, and table vibration.<sup>31,32</sup> To overcome this limitation, DTI sequences need to be as short as possible. In our study, we successfully proved the feasibility of accelerated DTI using SMS acquisition with blipped CAIPIRINHA.

A major challenge to DTI in general is the short T2 relaxation time of skeletal muscle (35 milliseconds at 3 T), which causes an inherently unfavorable SNR.<sup>18</sup> Slice acceleration leads to further decreasing SNR because of saturation effects (due to shorter TR) and growing g-factor penalty. However, there is a net gain in SNR per time unit as long as TR is longer than 1.25 T1.<sup>22</sup> Therefore, given the T1 relaxation time of 1412 (13) milliseconds in the skeletal muscle at 3 T,<sup>17</sup> the SNR per time unit can be expected to increase even with 3-fold slice acceleration (TR, 2100 milliseconds), which is confirmed by our results.

To optimize the SNR, we used a very short TE (54 milliseconds) and 5/8 partial Fourier sampling in all sequences. Furthermore, 2 signal averages and 20 gradient directions were acquired, which however extended the acquisition time. Previous studies on skeletal muscle used up to 16 signal averages but only 6 to 10 gradient directions.<sup>9,33–35</sup> We preferred a high number of gradient directions over additional signal averaging because a recent study found that DTI of skeletal muscle needs at least 12 gradient directions to be sufficiently accurate,<sup>26</sup> whereas other studies propose even 20 directions for robust estimation of anisotropy.<sup>36</sup> Signal averaging only elevates the SNR but has no

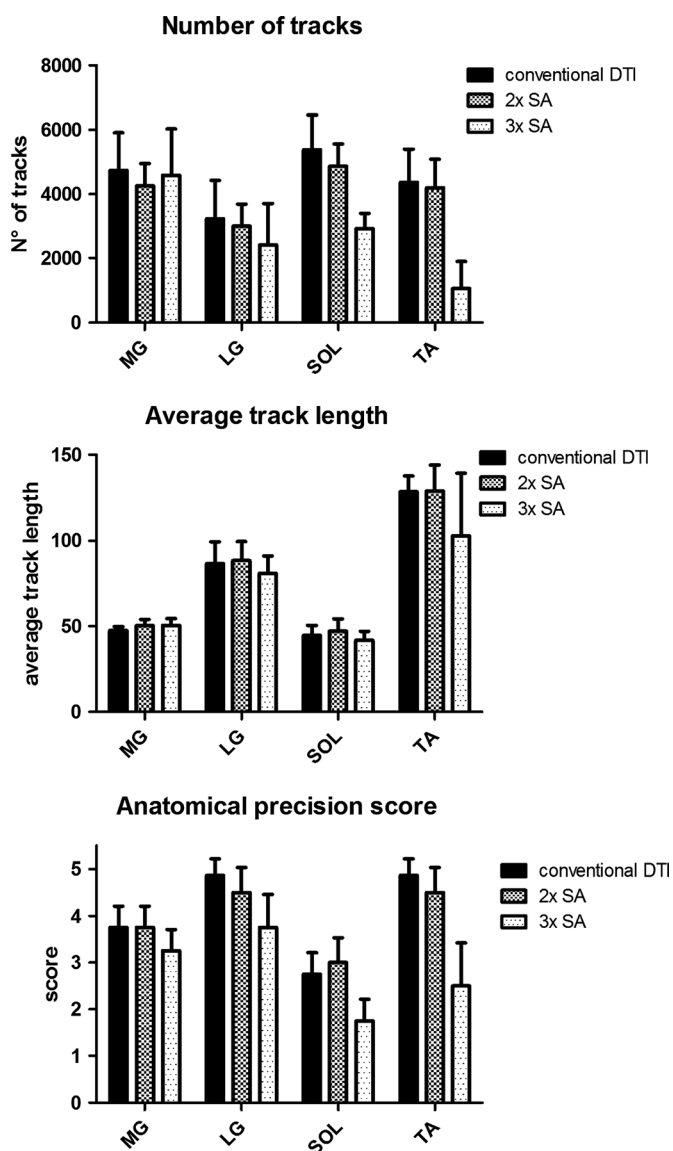


**FIGURE 4.** Performance of fiber tracking regarding the number of tracks, average track length (millimeter), and anatomical precision score. No significant differences were found between conventional DTI and 2-fold slice acceleration, whereas the number of tracks and the anatomical precision score significantly decreased in the soleus and TA muscles at 3-fold acceleration.

influence on the minimum sampling requirement of the diffusion tensor.<sup>37</sup> With the parameters used in our study, the SNR remained over the critical threshold of 25 for accurate muscle DTI<sup>26</sup> even at 3-fold slice acceleration (Table 2).

The SNR decreases exponentially with increasing  $b$  value. In most previous works on DTI of skeletal muscle, a  $b$  value between 400 and 600  $\text{s/mm}^2$  was applied.<sup>7,9,13,33,34,38–40</sup> As a compromise between SNR and sensitivity to diffusion as well as to achieve a short TE, we chose a  $b$  value of 500  $\text{s/mm}^2$ , which has proven the optimal value in a recent computer-based simulation study.<sup>26</sup> Fractional anisotropy and MD measured in the conventional DTI scan were in the range of previously reported values.<sup>7,9,13,31,33,41</sup> The observation that FA values were higher in the TA muscle than in the others may be explained with the slight plantar flexion (passive muscle elongation) during magnetic resonance examination.<sup>41</sup> No significant changes of DTI parameters were found at 2-fold slice acceleration. At 3-fold acceleration, however, the FA values were significantly higher compared with conventional DTI. This known phenomenon may be attributed to the reduced acquisition time per slice.<sup>25,42</sup> There was no notable influence of the slice acceleration factor on the variability and reproducibility of FA and MD measurements.

Fiber tracking allows 3-dimensional visualization of highly structured anisotropic tissues. This method was first validated in the skeletal muscle by Damon et al,<sup>6</sup> and its potential for characterizing muscle injuries and structural abnormalities has since been described in several studies.<sup>12,13,43,44</sup> Similar to previous studies, we used an FA threshold of 0.15 and an angulation threshold of 30 degrees,<sup>38</sup> which provided a good equilibrium between effective fiber tracking and anatomical accuracy. Conventional DTI and 2-fold slice acceleration showed comparable fiber tracking results. An interesting exception is the slightly higher (though not statistically significant) track length found with 2-fold acceleration compared with conventional DTI. This phenomenon may be explained by the higher voxelwise FA values in slice-accelerated sequences (see above), which causes more voxels to exceed the FA threshold for fiber tracking. At 3-fold slice acceleration, this effect was not observed anymore, most probably because of the lower SNR that caused fiber tracking to stop prematurely.

The average track lengths measured in this study need careful interpretation because some muscle fibers likely exceeded the field of view in the  $z$  direction (17.1 cm). This parameter was determined mainly for comparing the fiber tracking performance depending on slice acceleration rather than for exact determination of the fiber length from aponeurosis to aponeurosis. The latter is known to be already limited by image noise<sup>9</sup> and therefore not commonly reported in the literature. It has to be noted that the present study did not evaluate pennation angles of muscle fibers, which would have required more comprehensive fiber tracking methods with marking the aponeurosis and bundling muscle fibers with similar characteristics.<sup>6</sup> Nevertheless,

**TABLE 2.** SNR in the Different Muscle Groups at Different Slice Acceleration Factors

Muscle	Conventional DTI (No Slice Acceleration)		Two-Fold Slice Acceleration		Three-Fold Slice Acceleration	
	SNR	SNR/min	SNR	SNR/min	SNR	SNR/min
MG	65.63 (10.29)	8.87 (1.39)	55.18 (12.39)	14.21 (3.66)	43.49 (10.24)	16.52 (3.89)
LG	59.84 (5.11)	8.09 (0.69)	46.97 (10.67)	12.10 (3.12)	37.92 (8.05)	14.40 (3.06)
SOL	55.45 (7.12)	7.49 (1.01)	42.56 (11.21)	10.96 (2.82)	31.83 (7.77)	12.09 (2.95)
TA	48.32 (3.99)	6.53 (0.54)	36.29 (10.62)	9.35 (2.41)	27.24 (6.90)	10.35 (2.62)
Mean	57.31 (6.63)	7.74 (1.05)	45.25 (11.22)	11.65 (3.00)	35.12 (8.24)	13.34 (3.13)

Although the SNR decreased at higher slice acceleration, the SNR per minute (SNR/min) increased continuously.

SNR indicates signal-to-noise ratio; DTI, diffusion tensor magnetic resonance imaging; MG, medial head of gastrocnemius muscle; LG, lateral head of gastrocnemius muscle; SOL, soleus muscle; TA, tibialis anterior muscle.



because all other parameters were similar between conventional DTI and 2-fold slice acceleration, pennation angle measurements are not supposed to be altered.

Diffusion tensor magnetic resonance imaging of skeletal muscle is influenced by numerous factors, such as age, intramuscular fat content, or exercise. We believe that both conventional and accelerated DTI will be equally influenced by these factors. One exception is the fact that FA values increase with higher slice acceleration (although not significantly different in the present work). This might involve the use of different FA cutoff values to discriminate between healthy and pathological conditions.

There are limitations to this study. First, the true SNR was not measured because this is difficult in case of parallel imaging. Instead, an effective SNR was defined in accordance to previous studies, which proved a good approximation.<sup>28,29</sup> Second, the study population was relatively small; however, as there was excellent agreement between interindividual and intraindividual measurements, a larger population would most likely not have yielded much additional information for this feasibility study. Third, the experiments were only performed at 3 T. This field strength is advantageous over 1.5 T for musculoskeletal applications due to the higher signal yield. Although the lower SNR at 1.5 T might have slightly impaired image quality, it can be assumed that a slice acceleration factor of 2 would have been the best compromise as well.

In conclusion, SMS acquisition of diffusion tensor data is feasible and yields similar results as conventional DTI at notably shorter acquisition time. With the parameters used in the present study, an acceleration factor of 2 showed to be the best compromise between total acquisition time, image quality, and quantification accuracy. The higher SNR per time unit outweighs the disadvantage of the slightly lower SNR per excitation compared with conventional DTI. Future DTI studies on skeletal muscle may significantly benefit from this remarkable scan time reduction that increases the clinical applicability of this promising technique. It has to be investigated yet whether SMS acquisition qualifies for the assessment of pathologies such as muscle edema, tear, or hematoma,<sup>11–13</sup> where DTI seems to have its greatest potential for clinical application.

## ACKNOWLEDGMENTS

The authors kindly thank Himanshu Bhat (Siemens Medical Solutions USA Inc, Charlestown, MA) and Heiko Meyer (Siemens Healthcare, Erlangen, Germany) for providing them with the software for simultaneous multislice acquisition.

## REFERENCES

- Basser PJ, Mattiello J, LeBihan D. MR diffusion tensor spectroscopy and imaging. *Biophys J*. 1994;66:259–267.
- Bammer R, Acar B, Moseley ME. In vivo MR tractography using diffusion imaging. *Eur J Radiol*. 2003;45:223–234.
- Basser PJ, Pajevic S, Pierpaoli C, et al. In vivo fiber tractography using DT-MRI data. *Magn Reson Med*. 2000;44:625–632.
- Rohrer M, Sitek A, Gullberg GT. Reconstruction and visualization of fiber and laminar structure in the normal human heart from ex vivo diffusion tensor magnetic resonance imaging (DTMRI) data. *Invest Radiol*. 2007;42:777–789.
- Gasparotti R, Lodoli G, Meoded A, et al. Feasibility of diffusion tensor tractography of brachial plexus injuries at 1.5 T. *Invest Radiol*. 2013;48:104–112.
- Damon BM, Ding Z, Anderson AW, et al. Validation of diffusion tensor MRI-based muscle fiber tracking. *Magn Reson Med*. 2002;48:97–104.
- Galbán CJ, Maderwald S, Uffmann K, et al. Diffusive sensitivity to muscle architecture: a magnetic resonance diffusion tensor imaging study of the human calf. *Eur J Appl Physiol*. 2004;93:253–262.
- Heemskerk AM, Strijkers GJ, Vilanova A, et al. Determination of mouse skeletal muscle architecture using three-dimensional diffusion tensor imaging. *Magn Reson Med*. 2005;53:1333–1340.
- Sinha S, Sinha U, Edgerton VR. In vivo diffusion tensor imaging of the human calf muscle. *J Magn Reson Imaging*. 2006;24:182–190.
- Hiepe P, Herrmann KH, Güllmar D, et al. Fast low-angle shot diffusion tensor imaging with stimulated echo encoding in the muscle of rabbit shank. *NMR Biomed*. 2014;27:146–157.
- Fan RH, Does MD. Compartmental relaxation and diffusion tensor imaging measurements in vivo in lambda-carrageenan-induced edema in rat skeletal muscle. *NMR Biomed*. 2008;21:566–573.
- Zeng H, Zheng JH, Zhang JE, et al. Grading of rabbit skeletal muscle trauma by diffusion tensor imaging and tractography on magnetic resonance imaging. *Chin Med Sci J*. 2006;21:276–280.
- Zaraskaya T, Kumbhare D, Noseworthy MD. Diffusion tensor imaging in evaluation of human skeletal muscle injury. *J Magn Reson Imaging*. 2006;24:402–408.
- Froeling M, Oudeman J, Strijkers GJ, et al. Muscle changes detected by diffusion-tensor imaging after long-distance running. *Radiology*. 2015;274:548–562.
- Okamoto Y, Kemp GJ, Isobe T, et al. Changes in diffusion tensor imaging (DTI) eigenvalues of skeletal muscle due to hybrid exercise training. *Magn Reson Imaging*. 2014;32:1297–1300.
- Noehren B, Andersen A, Feiweier T, et al. Comparison of twice refocused spin echo versus stimulated echo diffusion tensor imaging for tracking muscle fibers. *J Magn Reson Imaging*. 2015;41:624–632.
- Stanisz GJ, Odorobina EE, Pun J, et al. T1, T2 relaxation and magnetization transfer in tissue at 3 T. *Magn Reson Med*. 2005;54:507–512.
- Damon BM. Effects of image noise in muscle diffusion tensor (DT)-MRI assessed using numerical simulations. *Magn Reson Med*. 2008;60:934–944.
- Pruessmann KP, Weiger M, Scheidegger MB, et al. SENSE: sensitivity encoding for fast MRI. *Magn Reson Med*. 1999;42:952–962.
- Feinberg DA, Crooks LE, Hoenninger JC, et al. Contiguous thin multisection MR imaging by two-dimensional Fourier transform techniques. *Radiology*. 1986;158:811–817.
- Breuer FA, Blaimer M, Heidemann RM, et al. Controlled aliasing in parallel imaging results in higher acceleration (CAPIRINHA) for multi-slice imaging. *Magn Reson Med*. 2005;53:684–691.
- Setsompop K, Gagoski BA, Polimeni JR, et al. Blipped-controlled aliasing in parallel imaging for simultaneous multislice echo planar imaging with reduced g-factor penalty. *Magn Reson Med*. 2012;67:1210–1224.
- Chang WT, Setsompop K, Ahveninen J, et al. Improving the spatial resolution of magnetic resonance inverse imaging via the blipped-CAPI acquisition scheme. *Neuroimage*. 2014;91:401–411.
- Eichner C, Jafari-Khouzani K, Cauley S, et al. Slice accelerated gradient-echo spin-echo dynamic susceptibility contrast imaging with blipped CAPI for increased slice coverage. *Magn Reson Med*. 2014;72:770–778.
- Lau AZ, Tunnicliffe EM, Frost R, et al. Accelerated human cardiac diffusion tensor imaging using simultaneous multislice imaging. *Magn Reson Med*. 2015;73:995–1004.
- Froeling M, Nederveen AJ, Nicolay K, et al. DTI of human skeletal muscle: the effects of diffusion encoding parameters, signal-to-noise ratio and T2 on tensor indices and fiber tracts. *NMR Biomed*. 2013;26:1339–1352.
- Schwenzer NF, Steidle G, Martirosian P, et al. Diffusion tensor imaging of the human calf muscle: distinct changes in fractional anisotropy and mean diffusion due to passive muscle shortening and stretching. *NMR Biomed*. 2009;22:1047–1053.
- Price RR, Axel L, Morgan T, et al. Quality assurance methods and phantoms for magnetic resonance imaging: report of AAPM nuclear magnetic resonance Task Group No. 1. *Med Phys*. 1990;17:287–295.
- Khalil C, Hancart C, Le Thuc V, et al. Diffusion tensor imaging and tractography of the median nerve in carpal tunnel syndrome: preliminary results. *Eur Radiol*. 2008;18:2283–2291.
- Landis JR, Koch GG. The measurement of observer agreement for categorical data. *Biometrics*. 1977;33:159–174.
- Saupe N, White LM, Sussman MS, et al. Diffusion tensor magnetic resonance imaging of the human calf: comparison between 1.5 T and 3.0 T-preliminary results. *Invest Radiol*. 2008;43:612–618.
- Karampinos DC, Banerjee S, King KF, et al. Considerations in high-resolution skeletal muscle diffusion tensor imaging using single-shot echo planar imaging with stimulated-echo preparation and sensitivity encoding. *NMR Biomed*. 2012;25:766–778.
- Galbán CJ, Maderwald S, Uffmann K, et al. A diffusion tensor imaging analysis of gender differences in water diffusivity within human skeletal muscle. *NMR Biomed*. 2005;18:489–498.
- Lansdown DA, Ding Z, Wadington M, et al. Quantitative diffusion tensor MRI-based fiber tracking of human skeletal muscle. *J Appl Physiol (1985)*. 2007;103:673–681.
- Heemskerk AM, Sinha TK, Wilson KJ, et al. Repeatability of DTI-based skeletal muscle fiber tracking. *NMR Biomed*. 2010;23:294–303.
- Jones DK. The effect of gradient sampling schemes on measures derived from diffusion tensor MRI: a Monte Carlo study. *Magn Reson Med*. 2004;51:807–815.



37. Papadakis NG, Murrills CD, Hall LD, et al. Minimal gradient encoding for robust estimation of diffusion anisotropy. *Magn Reson Imaging*. 2000;18:671–679.
38. Saupe N, White LM, Stainsby J, et al. Diffusion tensor imaging and fiber tractography of skeletal muscle: optimization of B value for imaging at 1.5 T. *AJR Am J Roentgenol*. 2009;192:W282–W290.
39. Budzik JF, Balbi V, Verclytte S, et al. Diffusion tensor imaging in musculoskeletal disorders. *Radiographics*. 2014;34:E56–E72.
40. Heemskerk AM, Sinha TK, Wilson KJ, et al. Quantitative assessment of DTI-based muscle fiber tracking and optimal tracking parameters. *Magn Reson Med*. 2009;61:467–472.
41. Deux JF, Malzy P, Paragios N, et al. Assessment of calf muscle contraction by diffusion tensor imaging. *Eur Radiol*. 2008;18:2303–2310.
42. Jones DK, Cercignani M. Twenty-five pitfalls in the analysis of diffusion MRI data. *NMR Biomed*. 2010;23:803–820.
43. Kan JH, Heemskerk AM, Ding Z, et al. DTI-based muscle fiber tracking of the quadriceps mechanism in lateral patellar dislocation. *J Magn Reson Imaging*. 2009;29:663–670.
44. Cermak NM, Noseworthy MD, Bourgeois JM, et al. Diffusion tensor MRI to assess skeletal muscle disruption following eccentric exercise. *Muscle Nerve*. 2012;46:42–50.